Vol. 215, No. 1, 1995 BIOCHEMICAL AND BIOPHYSICAL RESEARCH COMMUNICATIONS
October 4, 1995 Pages 264-271

STRUCTURE OF PREJUNCTIONAL RECEPTOR BINDING ANALOG OF HUMAN NEUROPEPTIDE Y DIMER ANA-NPY

Julian A. Barden

Department of Anatomy and Histology, The University of Sydney, Sydney NSW 2006,Australia

Received August 20, 1995

SUMMARY: Human neuropeptide Y (NPY) analog ANA-NPY or [L17, Q19, A20, A23, L28, L31]NPY(13-36)-amide binds weakly to postjunctional receptors to raise blood pressure but binds tightly to prejunctional receptors to inhibit neurotransmitter release. ANA-NPY forms a well-conserved anti-parallel helical structure overlapping E23-Y36 with strong amphipathic character. The C-terminal portions of the monomers are better defined than the N-terminal ends. The N-terminal helices extend only from D16-E23/L24. The prejunctional receptor-specific binding site is confined within the C-terminal helices while the residues responsible for partial binding to the postjunctional receptors are located in the more disordered N-terminal segments.

Neuropeptide Y (NPY) raises blood pressure by binding to post-junctional or Y_1 receptors (1-4) and inhibits cardiac vagal action (5) by binding to prejunctional or Y_2 receptors which inhibits the release of the neurotransmitters acetylcholine (3, 6) and noradrenaline (7).

The structure of human NPY recently was determined using NMR spectroscopy (8, 9). Two contiguous C-terminal helices extending from residues 15-26 and 28-35 were revealed. The structure of the C-terminal region was found to be of particular interest when NPY peptides were produced which predominantly displayed prejunctional activity and only partial pressor or postjunctional activity (10). The NPY analog N-acetyl[L28, L31]NPY(24-36)-amide (11) inhibited cardiac vagal activity without manifesting residual pressor activity and is thus selectively capable of acting on the Y_2 receptor subtypes expressed on the human neuroblastoma cell line SK-N-MC. The structure determination revealed that the selective prejunctional peptide agonist adopted a single amphipathic helical conformation extending from 24-34 very similar to the structure of the same region in the full-length peptide (12).

The N-terminal extended peptide ANA-NPY binds strongly to Y_2 receptors on SMS-KAN cells with an IC_{50} of 7.3 ± 0.7 nM, very similar to that of the smaller selective prejunctional agonist (11), whereas both analogs show little binding to Y_1 receptors. However, ANA-NPY still retains significant

0006-291X/95 $12.00

pressor effects *in vivo* indicating that part of the N-terminal structure is involved in binding to Y_1 receptors. The structure of the ANA-NPY dimer is determined and compared with the packing of the intact molecule containing both receptor binding sites.

MATERIALS AND METHODS

ANA-NPY was synthesized and purified with the results confirmed using mass spectroscopy as described (11).

Proton NMR Spectroscopy. ANA-NPY was dissolved in 80% H_2O/ 20% F_3EtOH-d_2 at 4 mM, pH 3.7 and 293 K. Spectra were recorded at 400 MHz using a Bruker AMX-400 spectrometer without sample spinning. TOCSY (mixing time 120 ms with 2.5 ms trim pulses) (13, 14) experiments were used to assign spin systems (64 transients, 512 increments collected in 4 K data points). The residual water resonance was suppressed (12). NOESY (15) experiments were recorded with mixing times ranging from 150-300 ms (192 transients, 512 increments collected in 4 K points in F2). A 200 ms mix was used to derive proton-proton distance constraints. Data were zero-filled to 4 x 1 K and apodized using Gaussian multiplication in F2 (line broadening of -18 Hz and GB of 0.18) and shifted sine-bell in F1 (2) prior to Fourier transformation. Third-order polynomial functions were employed to correct baselines. Chemical shift was referenced to trimethylsilylpropanesulfonic acid.

Distance Geometry Calculations. Strong NOEs were assigned an upper distance constraint of 0.3 nm, medium NOEs 0.35 nm, medium weak NOEs 0.4 nm and weak NOEs 0.45 nm. Pseudoatom corrections were applied where stereospecific identification was not obtained. Torsion angles (ϕ) were constrained within the range -90° to -30° for all values of the coupling constant $^3J_{\alpha CHNH}$ less than 5 Hz. These were measured using high-resolution 1D spectra or COSY(8 K spectra). 2000 distance geometry structures were calculated from random starting structures using DIANA (16) on a Silicon Graphics R4000 workstation. The 15 structures with the lowest penalty values were refined in X-PLOR 3 using a dynamic simulated annealing method (17). The initial stage of the simulation involved 2000 cycles of energy minimization. Standard parameters were used to constrain covalent geometry (12). Refined structures had no angle violations nor any distance violations exceeding 5 pm. Molecular graphics were processed using INSIGHT II operating on a Silicon Graphics Indigo 2 workstation.

RESULTS

Assigning monomeric ANA-NPY was a straitforward task given the existing assignment of [L28, L31]NPY(24-36)-amide (12) together with the contributions from the N-terminal extension 13-23. However, the existence of a dimeric ANA-NPY structure forming under similar conditions was apparent, with a doubling of the number of cross peaks originating from the segment 24-36. Each set of connectivities exhibited closely similar intensity showing that the peptide formed essentially all dimer under the conditions. TOCSY, COSY and NOESYspectra were required to identify all the separate spin systems and to establish all the connectivities. The unique Pro13, Asp16, His26 and Thr32 spin systems could be assigned sequence-specifically from the TOCSY spectrum. NOESY correlations between sequential residues were used to specifically assign the remaining spin systems. The helical nature of the neuropeptides made some aspects of the otherwise complicated assignment

easier. An example of the sequential connectivities in the backbone amide region is shown in Fig. 1. A strong pattern of NH_i/NH_{i+1} connectivities is observed in both monomers with the connectivities of monomer **a** labeled above the diagonal while those specifically from monomer **b** are shown below. The complete list of chemical shifts in the dimer labeled as monomers **a** and **b** is shown in Table I.

Figure 2 summarizes only the regular sequential and short-range inter-residue backbone NOE information with the relative intensity of the NOE represented by the line thickness. The presence of strong NH_i/NH_{i+1} and medium $H\beta_i/NH_{i+1}$, $H\alpha_i/NH_{i+3}$ and $H\alpha_i/H\beta_{i+3}$ combined with weak or absent $H\alpha_i/NH_{i+1}$ connectivities indicate the presence of a helical structure in the region (18). Many other sequential and medium-range NOEs were measured between side chain protons up to 4 residues apart. The bottom row of NOEs refer to inter-monomer connectivities. These reveal that the monomers pack in an anti-parallel fashion with Tyr36 on monomer **a** close to Leu24 on monomer **b** and vice versa.

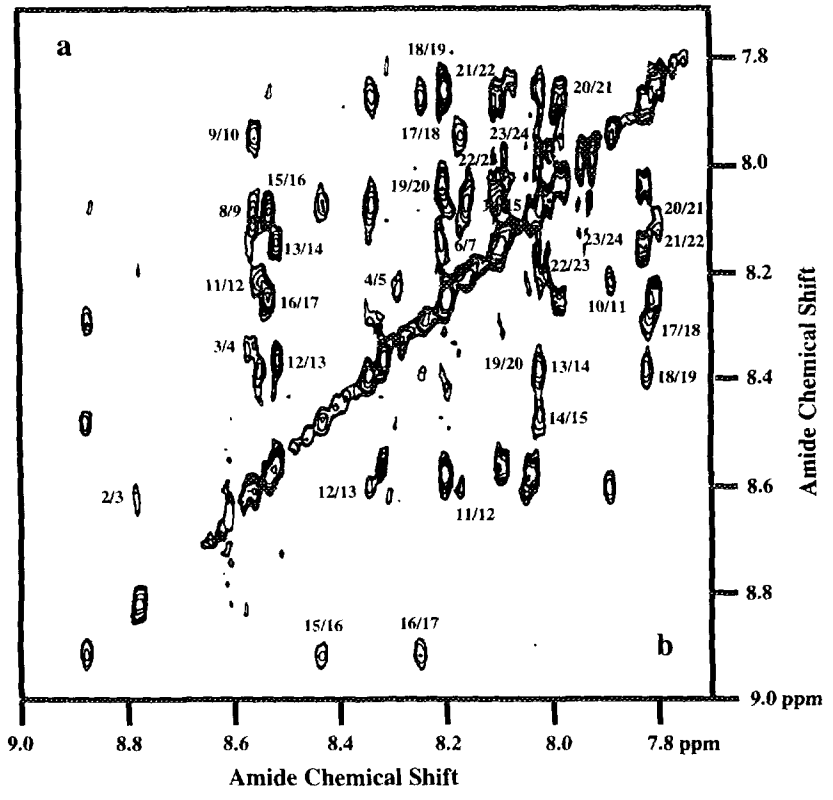

Figure 1. Expansion of a NOESY spectrum (τ_m = 200 ms) of ANA-NPY in 20% TFE-d_2/water at 293 K. The sequential pathway from monomer **a** is shown above the diagonal while those additional connectivities from monomer **b** are below the diagonal.

TABLE I: ^{1}H NMR Chemical Shifts (ppm) of human ANA-NPY dimer in 20% F_3EtOH-d_2. Monomers are labeled **a** and **b** where assignments differ

residue	NH	αH	βH	others
Pro13	-	4.39	2.49, 2.11	γCH$_2$ 2.10, 2.08; δCH$_2$ 3.48, 3.38
Ala14	8.78	4.31	1.43	
Glu15	8.66	4.28	2.02, 1.98	γCH$_2$ 2.38, 2.36
Asp16	8.25	4.62	2.81, 2.79	
Leu17	8.17	4.22	1.75, 1.73	γCH 1.59; δCH$_3$ 0.97, 0.90
Ala18	8.15	4.14	1.49	
Gln19	8.05	4.04	2.12, 2.08	γCH$_2$ 2.42, 2.35; δNH$_2$ 7.47, 6.78
Tyr20	8.22	4.23	3.14, 3.13	C2,6H 7.08; C3,5H 6.79
Ala21	8.44	4.04	1.51	
Ala22	7.90	4.09	1.53	
Glu23**a**	8.33	4.28	2.00, 1.98	γCH$_2$ 2.33, 2.31
Glu23**b**	8.18	4.10	2.28, 2.14	γCH$_2$ 2.57, 2.43
Leu24**a**	8.31	4.23	1.64, 1.62	γCH 1.66; δCH$_3$ 0.98, 0.92
Leu24**b**	8.47	4.17	1.60, 1.56	γCH 1.68; δCH$_3$ 0.89, 0.88
Arg25**a**	8.45	4.04	1.82, 1.78	γCH$_2$ 1.66, 1.62; δCH$_2$ 3.19, 3.17; NH 7.22
Arg25**b**	8.29	3.93	1.98, 1.93	γCH$_2$ 1.59, 1.57; δCH$_2$ 3.22, 3.20; NH 7.25
His26**a**	8.13	4.49	3.24, 3.21	2H 8.54; 4H 7.09
His26**b**	8.00	4.41	3.50, 3.32	2H 8.58; 4H 7.01
Tyr27**a**	8.04	4.33	3.14, 3.08	C2,6H 7.09; C3,5H 6.80
Tyr27**b**	8.36	4.20	3.19, 3.17	C2,6H 7.07; C3,5H 6.78
Leu28**a**	8.43	4.06	1.78, 1.74	γCH 1.51; δCH$_3$ 0.90, 0.87
Leu28**b**	8.79	3.94	1.89, 1.86	γCH 1.51; δCH$_3$ 0.88, 0.85
Asn29**a**	8.19	4.48	2.92, 2.82	δNH$_2$ 7.54, 6.89
Asn29**b**	8.24	4.40	2.99, 2.80	δNH$_2$ 7.57, 6.89
Leu30**a**	7.86	4.10	1.79, 1.59	γCH 1.80; δCH$_3$ 0.86, 0.84
Leu30**b**	7.80	4.02	1.83, 1.78	γCH 1.56; δCH$_3$ 0.82, 0.78
Leu31**a**	8.13	4.11	1.70, 1.67	γCH 1.55; δCH$_3$ 0.86, 0.84
Leu31**b**	8.25	4.01	1.54, 1.47	γCH 1.66; δCH$_3$ 0.89, 0.74
Thr32**a**	7.93	4.35	4.13	γCH$_3$ 1.28
Thr32**b**	7.98	4.40	4.07	γCH$_3$ 1.30
Arg33**a**	7.86	4.19	1.94, 1.88	γCH$_2$ 1.88, 1.70; δCH$_2$ 3.19, 3.17; NH 7.21
Arg33**b**	7.77	4.18	1.96, 1.93	γCH$_2$ 1.77, 1.72; δCH$_2$ 3.19, 3.18; NH 7.22
Gln34**a**	8.10	4.15	2.09, 2.05	γCH$_2$ 2.41, 2.33; δNH$_2$ 7.38, 6.75
Gln34**b**	8.11	4.18	2.10, 2.05	γCH$_2$ 2.39, 2.37; δNH$_2$ 7.34, 6.73
Arg35**a**	7.98	4.15	1.68, 1.65	γCH$_2$ 1.42, 1.38; δCH$_2$ 3.06, 3.04; NH 7.11
Arg35**b**	8.04	4.17	1.70, 1.66	γCH$_2$ 1.45, 1.37; δCH$_2$ 3.06, 3.04; NH 7.11
Tyr36**a**	7.95	4.58	3.15, 2.88	C2,6H 7.18; C3,5H 6.83
Tyr36**b**	7.92	4.58	3.19, 2.89	C2,6H 7.18; C3,5H 6.83

360 distance constraints and 14 angle constraints in each monomer (Leu17-Ala22, Leu24-Asn29 and Leu31-Thr32) were used in the distance geometry algorithm DIANA. Starting structures were created by connecting two identical monomers with a chain of 13 sterically transparent Gly residues. Calculations yielded 15 structures satisfying all distance (<5 pm) and angle constraints. These were refined using a dynamic simulated annealing protocol in XPLOR 3 with a simulation time of 75 ps (12). The family of refined structures was compared and the root mean square deviation of backbone atoms

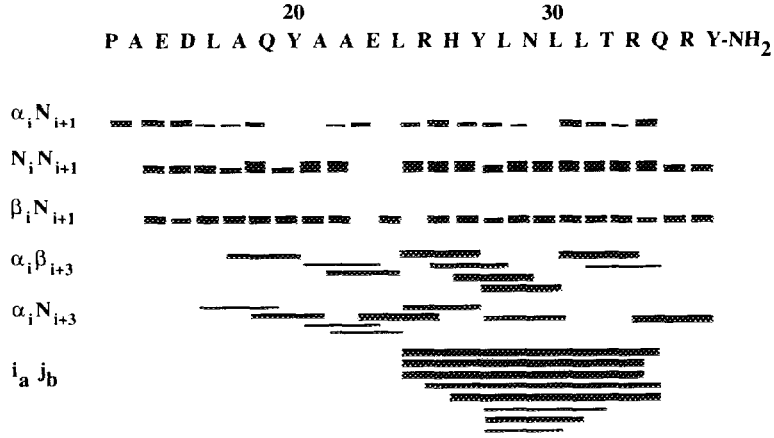

Figure 2. Summary of interresidue NOE data observed for ANA-NPY. The relative size of the connecting bars represent the NOE intensity.

measured throughout the molecule. A Lennard-Jones potential of -251±4 kJ.mol^{-1} demonstrated good non-bonded contacts. A degree of variability in the ϕ and ψ angles in the segments Pro13-Leu17 and Gln34-Tyr36 reflected some conformational averaging at both ends but particularly at the N-termini. Ramachandran plots of the dihedral angles indicated that the backbone angles were in allowed ranges. Consequently, calculation of the rms deviation in backbone atoms in each of the monomer segments was confined to Asp16-Tyr36. Monomer **a** yielded an rmsd of 75±3 pm while monomer **b** yielded an rmsd of 108±6 pm, with the C-terminus being the source of the extra averaging. A view of the 15 refined superimposed backbone structures is shown in Fig. 3. A total of 5 complete turns of helix is apparent with monomer **a** appearing the more constrained of the two presumably because of the extra constraint imposed on the C-terminus by the interaction with the other monomer. This

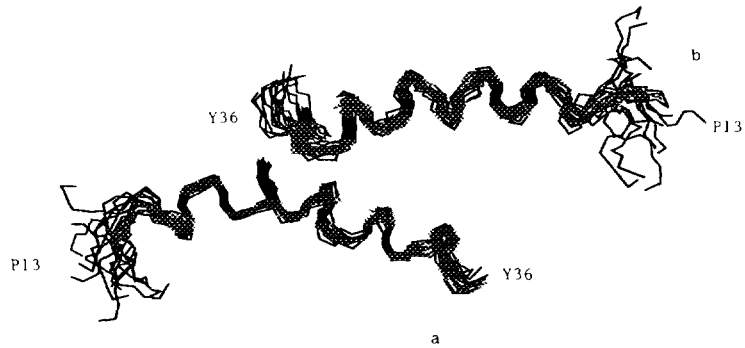

Figure 3. View of the backbone atoms of 15 refined structures of the ANA-NPY dimer superimposed over both segments Asp16-Tyr36. The monomers are arranged in an anti-parallel orientation overlapped at an interface in the segment Leu24-Tyr36, the segment containing the Y_2 receptor binding site.

close interaction is best seen in Fig. 4 where several of the side chains involved in stabilizing the dimer are shown.

DISCUSSION

A largely helical conformation is evident for the global fold of the convergent set of dimeric structures. As is often the case in protein helices, there is a well-defined hydrophobic face on the ANA-NPY helix, which is amphipathic in character. The refined structure of the monomers is similar to the same region in the full-length native NPY (8, 9, 18). However, one difference between the dimer structure involves the packing angle. ANA-NPY is found to dimerize in a much more regular anti-parallel orientation than was inferred from some of the NMR data from NPY in which the packing was more orthogonal (9). Because the spin systems of each ANA-NPY monomer in the overlap region are distinct, the dimer interactions could be measured directly and not simply modelled. Both ANA-NPY and the shorter stabilized N-acetyl[L28, L31]NPY(24-36)-amide (12) bind as well as NPY(1-36) to Y_2 receptors (11) but exhibit considerable conformational averaging in water. Their structures must be the same as the identical segments within NPY(1-36). Thus both shorter active peptides need to rely upon appropriate solvent environments to enable them to adopt their preferred solution structures. It is therefore necessary to provide an artificial hydrophobic environment which mimicks the environment in the vicinity of the peptide-receptor interface. To this end either micellar solutions or some aqueous organic solvents are used. These have been shown to stabilize structures in a similar way (19, 20). TFE stabilizes helical regions (21) as well as β-turns and β-sheet structures, yhe latter provided the segment is sufficiently long and not normally stabilized by other missing structures (21, 22). While most early studies on the effect of TFE

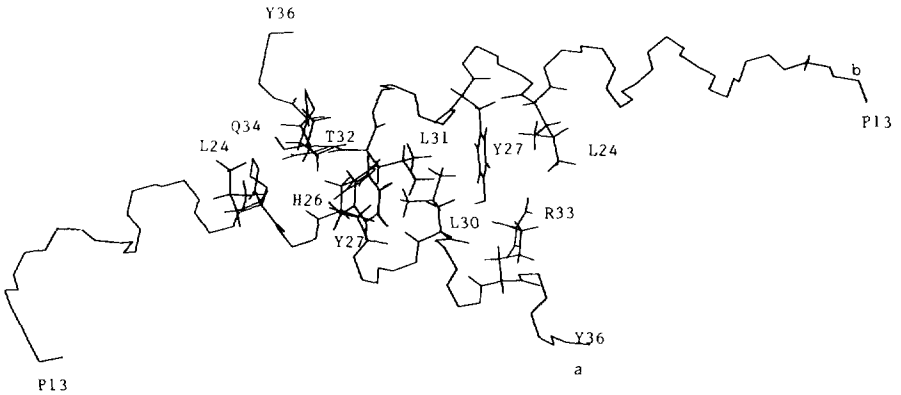

Figure 4. View of the backbone atoms of a single structure with the side chains of residues located at the interface.

on peptide structure used peptides from helical regions of proteins, it was not surprising that TFE was assumed to induce helix even in non-helical peptides. However, even high concentrations of TFE appear unable to induce helix in segments which are unordered in the native protein (21) and low concentrations of TFE have stabilized helix, turn and unordered structures in PTH and PTHrP (23, 24). Thus, TFE was again employed in this study to investigate both the structure of and packing in the ANA-NPY dimer.

ANA-NPY retains only a small amount of pressor-potentiating activity activity, being far less potent than NPY(13-36) (11). The amino acid substitutions in the N-terminal segment 13-23 do not alter the global fold of the peptide but do increase structural stability. It may be the increased stability or specific amino acid substitutions which reduce Y_1 receptor binding capacity. Both ANA-NPY and a structurally disturbed fragment des-Ser22-NPY(13-36) bind equally poorly to Y_1 receptors (10). Thus, it may be the specific amino acid substitutions at positions 17, 19, 20 and 23 in the segment 13-23 which causes partial loss of affinity. Both these peptides have equal potency in binding Y_2 receptors (10) indicating that the conformations of the C-terminal portion of the amphipathic helix from 24-36 are identical. Prejunctional receptor binding is confined to this C-terminal amphipathic α-helix while postjunctional receptor binding must at least partially involve the Pro-rich disordered segment 1-12 as well as interactions with some residues in the helical segment 13-23. The report (9) that cross-linked NPY dimers remain active presumably indicates that the Y_1 receptor binding site remains available at either end of the cross-linked species without necessarily assuming that the receptors normally bind dimers.

ACKNOWLEDGMENTS

This research was supported by grants from the National Health and Medical Research Council of Australia. I wish to thank Dr. Erica K. Potter and Albert Tseng for many helpful discussions.

REFERENCES

1. Dahlöff, C., Dahlöff, P. and Lundberg, J. M. (1985) Eur. J. Pharmacol. 109, 289-292.
2. Potter, E. K. (1985) Neurosci. Lett. 54, 117-121.
3. Revington, M. L., Potter, E. K. and McCloskey, D. I. (1987) Clin. Exp. Pharmacol. Physiol. 14, 703-710.
4. Potter, E. K. and McCloskey, M. J. D. (1992) Neurosci. Lett. 134, 183-186.
5. Lehmann, J. (1990) Drug Dev. Res. 19, 329-351.
6. Warner, M. and Levy, M. N. (1989) Circ. Res. 64, 882-890.
7. Edvinsson, L. (1988) ISI Atlas of Science: Pharmacology 2, 357-361.
8. Darbon, H., Bernassau, J. -M., Deleuze, C., Chenu, J., Roussel, A. and Cambillau, C. (1992) Eur. J. Biochem. 209, 765-771.
9. Cowley, D. J., Hoflack, J. M., Pelton, J. T. and Saudek, V. (1992) Eur. J. Biochem. 205, 1099-1106.

10. Potter, E. K., Mitchell, L., McCloskey, M. J. D., Tseng, A., Goodman, A. E., Shine, J. and McCloskey, D. I. (1989) Regul. Pept. 25, 167-177.
11. Potter, E. K., Barden, J. A., McCloskey, M. J. D., Selbie, L. A., Tseng, A., Herzog, H. and Shine, J. (1994) Eur. J. Pharmacol. 267, 253-262.
12. Barden, J.A., Cuthbertson, R.M., Potter, E.K., Selbie, L.A. and Tseng, A. (1994) Biochim. Biophys. Acta 1206, 191-196.
13. Bax, A. and Davis, D. G. (1985) J. Magn. Res. 65, 355-360.
14. Griesinger, C., Otting, G., Wüthrich, K. and Ernst, R.R. (1988) J. Am. Chem. Soc. 110, 7870-7872.
15. Kumar, A., Ernst, R.R. and Wüthrich, K. (1980) Biochem. Biophys. Res. Commun. 64, 2229-2246.
16. Güntert, P. Braun, W. and Wüthrich, K. (1991) J. Mol. Biol. 217, 517-530.
17. Nilges, M., Clore, G. M. and Gronenborn, A. M. (1988) FEBS Lett. 239, 129-136.
18. Saudek, V. and Pelton, J. T. (1990) Biochemistry 29, 4509-4515.
19. Mammi, S. and Peggion, E. (1990) Biochemistry 29, 5265-5269.
20. Motta, A., Pastore, A., Goud, N.A. and Castiglione Morelli, M.A. (1991) Biochemistry 30, 10444-10450.
21. Sönnichsen, F.D., Van Eyk, J.E., Hodges, R.S. and Sykes, B.D. (1992) Biochemistry 31, 8790-8798.
22. Martenson, R.E., Park, J.Y. and Stone, A.L. (1985) Biochemistry 24, 7689-7695.
23. Barden, J.A. and Kemp, B.E. (1993) Biochemistry 32, 7126-7132.
24. Barden, J.A. and Kemp, B.E. (1994) Biochim. Biophys. Acta 1208, 256-262.